

Homological mirror symmetry for toric orbifolds of toric del Pezzo surfaces

Kazushi Ueda and Masahito Yamazaki

Abstract

We formulate a conjecture which describes the Fukaya category of an exact Lefschetz fibration defined by a Laurent polynomial in two variables in terms of a pair consisting of a consistent dimer model and a perfect matching on it. We prove this conjecture in some cases, and obtain homological mirror symmetry for quotient stacks of toric del Pezzo surfaces by finite subgroups of the torus as a corollary.

1 Introduction

The lattice of vanishing cycles equipped with the intersection form is called the *Milnor lattice*. It is a fundamental object in singularity theory, which is related to other fields of mathematics such as generalizations of root systems (see e.g. [21]) and monodromy of hypergeometric functions. The Milnor lattice admits a categorification called the *Fukaya category of Lefschetz fibration*, defined by Seidel [23] based on an idea of Kontsevich [19]. It is an A_∞ -category whose set of objects is a distinguished basis of vanishing cycles and whose spaces of morphisms are Lagrangian intersection Floer complexes. Although they are important invariants in singularity theory, it is often difficult to compute the Milnor lattice of a holomorphic function, let alone its Fukaya category.

Recent advances in string theory have given a significant progress in the case of Laurent polynomials in two variables. For a Laurent polynomial

$$W(x, y) = \sum_{(i, j) \in \mathbb{Z}^2} a_{ij} x^i y^j,$$

its Newton polygon $\Delta \subset \mathbb{R}^2$ is defined as the convex hull of $(i, j) \in \mathbb{Z}^2$ such that $a_{ij} \neq 0$;

$$\Delta := \text{Conv}\{(i, j) \in \mathbb{Z}^2 \mid a_{ij} \neq 0\}.$$

We always assume that the origin is in the interior of Δ . With a convex lattice polygon containing the origin in its interior, one can associate a pair (G, D) consisting of a *consistent dimer model* G and a *perfect matching* D on G . Dimer models are introduced by string theorists to study supersymmetric gauge theory in four dimensions [9, 10, 11, 13, 14, 15]. The pair (G, D) encodes the information of a directed A_∞ -category \mathcal{A}^\rightarrow described in [12]. Motivated by Feng, He, Kenaway and Vafa [8], we formulate the following conjecture:

Conjecture 1.1. *For a convex lattice polygon Δ containing the origin in its interior, there exist*

- a Laurent polynomial W whose Newton polygon coincides with Δ , and
- a pair (G, D) consisting of a consistent dimer model and a perfect matching on it, whose characteristic polygon coincides with Δ

such that one has a quasi-equivalence

$$\mathcal{A}^\rightarrow \cong \mathfrak{Fuk} W \quad (1.1)$$

of A_∞ -categories.

With a convex lattice polygon Δ containing the origin in its interior, one can associate a two-dimensional toric Fano stack X . If Δ is the characteristic polygon of a pair (G, D) , then one has an equivalence

$$D^b \mathcal{A}^\rightarrow \cong D^b \text{coh } X \quad (1.2)$$

of triangulated categories [16, 12]. By combining the equivalences (1.1) and (1.2), one obtains homological mirror symmetry

$$D^b \text{coh } X \cong D^b \mathfrak{Fuk} W \quad (1.3)$$

conjectured by Kontsevich [18, 19] as a corollary.

Now consider the pull-back

$$\widetilde{W} = W \circ \exp : \mathbb{C}^2 \rightarrow \mathbb{C}$$

of W by the universal cover

$$\exp : \mathbb{C}^2 \rightarrow (\mathbb{C}^\times)^2$$

of the torus. The fact that \widetilde{W} has infinitely many critical points for a given critical value does not cause any problem, and one can define the Fukaya category $\mathfrak{Fuk} \widetilde{W}$ of \widetilde{W} . We formulate Conjecture 6.2 in Section 6, which is slightly stronger than Conjecture 1.1 and implies a torus-equivariant version of homological mirror symmetry for two-dimensional toric Fano stacks:

Theorem 1.2. *If Conjecture 6.2 holds for a lattice polygon Δ , then there is an equivalence*

$$D^b \text{coh}^\mathbb{T} X \cong D^b \mathfrak{Fuk} \widetilde{W} \quad (1.4)$$

of triangulated categories, where \mathbb{T} is the algebraic torus acting on X and $D^b \text{coh}^\mathbb{T} X$ is the derived category of \mathbb{T} -equivariant coherent sheaves on X .

Equivariant homological mirror symmetry (1.4) for X implies homological mirror symmetry for the quotient stack $[X/A]$ of X by a finite subgroup A of the torus \mathbb{T} :

Theorem 1.3. *If Conjecture 6.2 holds for a lattice polygon Δ , then homological mirror symmetry*

$$D^b \text{coh } X \cong D^b \mathfrak{Fuk} W$$

holds for any lattice polygon $\phi(\Delta)$ obtained from Δ by an integral linear transformation $\phi : \mathbb{Z}^2 \rightarrow \mathbb{Z}^2$ of rank two.

We prove the following in this paper:

Theorem 1.4. *Conjecture 6.2 holds for lattice polygons corresponding to toric del Pezzo surfaces.*

This implies homological mirror symmetry for toric orbifolds of toric del Pezzo surfaces. The equivalence (1.3) is proved for \mathbb{P}^2 and $\mathbb{P}^1 \times \mathbb{P}^1$ by Seidel [22], weighted projective planes and Hirzebruch surfaces by Auroux, Katzarkov and Orlov [4], and toric del Pezzo surfaces by Ueda [26]. See also Auroux, Katzarkov and Orlov [3] for homological mirror symmetry for not necessarily toric del Pezzo surfaces, Abouzaid [1, 2] for an application of tropical geometry to homological mirror symmetry, and Kerr [17] for the behavior of homological mirror symmetry under weighted blowup of toric surfaces. Slightly different versions of homological mirror symmetry for toric stacks are proved by Fang, Liu, Treumann and Zaslow [5, 6, 7] and by Futaki and Ueda [12].

The organization of this paper is as follows: We collect basic definitions and facts on dimer models and A_∞ -categories in Section 2. Toric Fano stacks associated with lattice polygons are recalled in Section 3, and Fukaya categories of exact Lefschetz fibrations are recalled in Section 4. In Section 5, we discuss homological mirror symmetry for \mathbb{P}^2 proved by Seidel [22] from a coamoeba point of view. This motivates Conjecture 6.2 in Section 6, which is shown to imply torus-equivariant homological mirror symmetry in Section 7. The proof of Theorem 1.4 is given in Section 8.

Acknowledgment: K. U. thanks Alastair Craw and Akira Ishii for valuable discussions. K. U. is supported by Grant-in-Aid for Young Scientists (No.18840029).

2 Dimer models and A_∞ -categories

We first recall basic definitions on dimer models:

- A *dimer model* is a bicolored graph $G = (B, W, E)$ on an oriented real 2-torus, which divides the torus into polygons. Here B is the set of black nodes, W is the set of white nodes, and E is the set of edges. No edge is allowed to connect nodes with the same color.
- A *quiver* consists of a finite set V called the set of vertices, another finite set A called the set of arrows, and two maps $s, t : A \rightarrow V$ called the source and the target map. The quiver $Q = (V, A, s, t)$ associated with G is defined as the dual graph of G , equipped with the orientation so that the white node is always on the right of an arrow; the set V of vertices is the set of faces of G , and the set A of arrows can naturally be identified with the set E of edges of G .
- A *perfect matching* is a subset $D \subset E$ such that for any $n \in B \sqcup W$, there is a unique edge $e \in D$ adjacent to n . A dimer model is *non-degenerate* if for any edge $e \in E$, there is a perfect matching D such that $e \in D$.
- A perfect matching D is said to be *internal* if there is a choice of a total order $>$ on the set of vertices of the quiver Q such that

$$D = \{a \in A \mid s(a) < t(a)\} \subset A = E. \quad (2.1)$$

- A non-degenerate dimer model is *consistent* if it satisfies the conditions in [20, Lemma 4.11].

Next we recall the definition of an A_∞ -category: An A_∞ -category \mathcal{A} consists of

- a set $\mathfrak{Ob}(\mathcal{A})$ of objects,
- for $c_1, c_2 \in \mathfrak{Ob}(\mathcal{A})$, a \mathbb{Z} -graded vector space $\text{hom}_{\mathcal{A}}(c_1, c_2)$ called the space of morphisms, and
- operations

$$\mathbf{m}_l : \text{hom}_{\mathcal{A}}(c_{l-1}, c_l) \otimes \cdots \otimes \text{hom}_{\mathcal{A}}(c_0, c_1) \longrightarrow \text{hom}_{\mathcal{A}}(c_0, c_l)$$

of degree $2 - l$ for $l = 1, 2, \dots$ and $c_0, \dots, c_l \in \mathfrak{Ob}(\mathcal{A})$,

satisfying the A_∞ -relations

$$\sum_{i=0}^{l-1} \sum_{j=i+1}^l (-1)^{\deg a_1 + \cdots + \deg a_{i-j}} \mathbf{m}_{l+i-j+1}(a_l \otimes \cdots \otimes a_{j+1} \otimes \mathbf{m}_{j-i}(a_j \otimes \cdots \otimes a_{i+1}) \otimes a_i \otimes \cdots \otimes a_1) = 0, \quad (2.2)$$

for any positive integer l , any sequence c_0, \dots, c_l of objects of \mathcal{A} , and any sequence of morphisms $a_i \in \text{hom}_{\mathcal{A}}(c_{i-1}, c_i)$ for $i = 1, \dots, l$.

Let $G = (B, W, E)$ be a dimer model and $Q = (V, A, s, t)$ be the quiver associated with G . Then the A_∞ -category \mathcal{A} associated with G is defined as follows [12, Definition 2.1]:

- The set of objects is the set V of vertices of the quiver.
- For two objects v and w in \mathcal{A} , the space of morphisms is given by

$$\text{hom}^i(v, w) = \begin{cases} \mathbb{C} \cdot \text{id}_v & i = 0 \text{ and } v = w, \\ \text{span}\{a \mid a : w \rightarrow v\} & i = 1, \\ \text{span}\{a^\vee \mid a : v \rightarrow w\} & i = 2, \\ \mathbb{C} \cdot \text{id}_v^\vee & i = 3 \text{ and } v = w, \\ 0 & \text{otherwise.} \end{cases}$$

- Non-zero A_∞ -operations are

$$\mathbf{m}_2(x, \text{id}_v) = \mathbf{m}_2(\text{id}_w, x) = x$$

for any $x \in \text{hom}(v, w)$,

$$\mathbf{m}_2(a, a^\vee) = \text{id}_v^\vee$$

and

$$\mathbf{m}_2(a^\vee, a) = \text{id}_w^\vee$$

for any arrow a from v to w ,

$$\mathbf{m}_k(a_1, \dots, a_k) = a_0$$

for any cycle (a_0, \dots, a_k) of the quiver going around a white node, and

$$\mathbf{m}_k(a_1, \dots, a_k) = -a_0$$

for any cycle (a_0, \dots, a_k) of the quiver going around a black node.

For an A_∞ -category \mathcal{A} and a total order $<$ on the set of objects, the *directed subcategory* \mathcal{A}^\rightarrow is the A_∞ -category whose set of objects is the same as \mathcal{A} and whose spaces of morphisms are given by

$$\mathrm{hom}_{\mathcal{A}^\rightarrow}(X, Y) = \begin{cases} \mathbb{C} \cdot \mathrm{id}_X & X = Y, \\ \mathrm{hom}_{\mathcal{A}}(X, Y) & X < Y, \\ 0 & \text{otherwise,} \end{cases}$$

with the A_∞ -operations inherited from \mathcal{A} .

If (G, D) is a pair of a consistent dimer model G and an internal perfect matching D on G , then the directed subcategory \mathcal{A}^\rightarrow of \mathcal{A} does not depend on the choice of a total order $<$ on vertices of the quiver satisfying (2.1).

3 Toric Fano stacks associated with lattice polygons

Let $N = \mathbb{Z}^2$ be a free abelian group of rank two and $M = \mathrm{Hom}(N, \mathbb{Z})$ be the dual group. We write $N_{\mathbb{R}} = N \otimes \mathbb{R}$, $M_{\mathbb{R}} = M \otimes \mathbb{R}$ and $\mathbb{T} = N \otimes \mathbb{C}^\times = \mathrm{Spec} \mathbb{C}[M]$. Let Δ be a convex lattice polygon in $N_{\mathbb{R}}$ containing the origin in its interior, and $\{v_i\}_{i=1}^r$ be the set of vertices of Δ numbered in accordance with the cyclic order. Let

$$\varphi : \mathbb{Z}^r \rightarrow N$$

be the homomorphism of abelian groups sending the i -th standard coordinate $e_i \in \mathbb{Z}^r$ to $v_i \in N$ for $i = 1, \dots, r$. Then the toric Fano stack $X = X_\Delta$ associated with Δ is the quotient stack

$$X = [(\mathbb{C}^r \setminus \mathcal{SR})/\mathcal{K}]$$

of an open subscheme of \mathbb{C}^r by the natural action of

$$\mathcal{K} = \mathrm{Ker}(\varphi \otimes \mathbb{C}^\times : (\mathbb{C}^\times)^r \rightarrow \mathbb{T}),$$

where the Stanley-Reisner locus $\mathcal{SR} \subset \mathbb{C}^r$ is defined by

$$\mathcal{SR} = \{(x_1, \dots, x_r) \in \mathbb{C}^r \mid (x_i, x_j) \neq (0, 0) \text{ if } v_i \text{ and } v_j \text{ are not adjacent}\}$$

if $r > 3$, and consists of the origin if $r = 3$.

Let $\phi : N \rightarrow N$ be an endomorphism of rank two. Then the toric Fano stack associated with the polygon $\phi(\Delta)$ is the quotient stack

$$X_{\phi(\Delta)} = [X_\Delta/K]$$

of X_Δ by the group

$$K = \mathrm{Ker}(\phi \otimes \mathbb{C}^\times : \mathbb{T} \rightarrow \mathbb{T}).$$

It follows from [16, Theorem 7.2] and [12, Proposition 3.2] that for a pair (G, D) of a consistent dimer model and an internal perfect matching on it, there is a lattice polygon Δ containing the origin in its interior such that there is an equivalence

$$D^b \mathcal{A}^\rightarrow \cong D^b \text{coh } X_\Delta$$

of triangulated categories. The lattice polygon Δ is called the *characteristic polygon* of the pair (G, D) , and can be described in a combinatorial way in terms of *height changes* of perfect matchings.

4 Fukaya categories

Let W be a regular function on an algebraic torus $(\mathbb{C}^\times)^2 = \text{Spec } \mathbb{C}[x^{\pm 1}, y^{\pm 1}]$ equipped with an exact Kähler form

$$\omega = \frac{1}{2\sqrt{-1}} \left(\frac{dx \wedge d\bar{x}}{|x|^2} + \frac{dy \wedge d\bar{y}}{|y|^2} \right).$$

W is a *Lefschetz fibration* if all the critical points are non-degenerate with distinct critical values, and the horizontal lift $\tilde{\gamma}_x : [0, 1] \rightarrow X$ of a smooth path $\gamma : [0, 1] \rightarrow \mathbb{C}$ starting at $x \in p^{-1}(\gamma(0))$ is always defined. The latter condition is satisfied if the Newton polygon Δ of W contains the origin in its interior, and the leading term of W with respect to any edge of Δ has no critical point on the torus.

Assume that the origin is a regular value of W . A *distinguished basis of vanishing cycles* is a collection (C_1, \dots, C_m) of embedded circles in $W^{-1}(0)$ which collapse to critical points by parallel transport along a *distinguished set of vanishing paths*, cf. [25, Section 16]. We assume that vanishing cycles intersect each other transversely.

A *relative grading* of W is a nowhere-vanishing smooth section of the holomorphic line bundle $\Lambda^{\text{top}}(T^*(\mathbb{C}^\times)^2)^{\otimes 2} \otimes W^*(T^*\mathbb{C})^{\otimes (-2)}$, which we choose as $(d \log x \wedge d \log y)^{\otimes 2} \otimes (dW)^{\otimes (-2)}$. It induces a section η of $\Lambda^{\text{top}}(T^*M)^{\otimes 2}$ on the fiber $M = W^{-1}(0)$, which gives a map

$$\begin{array}{ccc} \det_\eta^2 : & \mathcal{Lag}_M & \rightarrow & \mathbb{C}^\times / \mathbb{R}^{>0} \cong S^1 \\ & \Downarrow & & \Downarrow \\ & \text{span}\{e_1, \dots, e_n\} & \mapsto & [\eta((e_1 \wedge \dots \wedge e_n)^{\otimes 2})] \end{array}$$

from the Lagrangian Grassmannian bundle \mathcal{Lag}_M on M . A Lagrangian submanifold $L \subset M$ naturally gives a section

$$\begin{array}{ccc} s_L : & L & \rightarrow & \mathcal{Lag}_M|_L \\ & \Downarrow & & \Downarrow \\ & x & \mapsto & T_x L. \end{array}$$

A grading of L is a lift $\tilde{\phi}_L : L \rightarrow \mathbb{R}$ of the composition

$$\phi_L = \det_\eta^2 \circ s_L : L \rightarrow S^1$$

to the universal cover $\mathbb{R} \rightarrow S^1$.

Given a pair (L_1, L_2) of graded Lagrangian submanifolds, one can define the *Maslov index* $\mu(x; L_1, L_2)$ for each intersection point $x \in L_1 \cap L_2$. Since $\dim_{\mathbb{C}} M = 1$, it is given by the round-up

$$\mu(x; L_1, L_2) = \lceil \tilde{\phi}_{L_2}(x) - \tilde{\phi}_{L_1}(x) \rceil$$

of the difference of the phase functions at x .

The Fukaya category $\mathfrak{Fuk} W$ of W is a directed A_{∞} -category whose set of object is $(C_i)_{i=1}^m$ and whose spaces of morphisms are given by

$$\text{hom}(C_i, C_j) = \begin{cases} \text{id}_{C_i} & i = j, \\ \bigoplus_{p \in C_i \cap C_j} \mathbb{C} \cdot p & i < j, \\ 0 & \text{otherwise.} \end{cases}$$

The A_{∞} -operation is given by

$$\mathbf{m}_k(p_k, \dots, p_1) = \sum_{p_0 \in \cap C_{i_k} \cap C_{i_0}} (-1)^{\dagger} p_0, \quad (4.1)$$

where $p_{\ell} \in C_{i_{\ell-1}} \cap C_{i_{\ell}}$ for $\ell = 1, \dots, k$ and the sum is over the ‘ $(k+1)$ -gons’ whose ℓ -th vertex is the point p_{ℓ} for $\ell = 0, \dots, k$ and whose edge between p_{ℓ} and $p_{\ell+1}$ lies on $C_{i_{\ell}}$. The grading of $C_{i_{\ell}}$ defines an orientation of $C_{i_{\ell}}$, and let ξ_{ℓ} , $\ell = 0, \dots, k$ be the unit tangent vector of $C_{i_{\ell}}$ at p_{ℓ} along the orientation. We also choose a branch point on each vanishing cycle $C_{i_{\ell}}$, which comes from the choice of the non-trivial spin structure. In this paper, we only deal with the case where $\mu(p_{\ell}; C_{i_{\ell-1}}, C_{i_{\ell}}) = 1$ for $\ell = 1, \dots, k$ and $\mu(p_0; C_{i_0}, C_{i_k}) = 2$. In this case, the sign rule of Seidel [24, Section (9e)] states that \dagger in (4.1) is the sum of (i) the number of $1 \leq \ell \leq k$ such that ξ_{ℓ} points away from the $(k+1)$ -gon, and (ii) the the number of branch points on the $(k+1)$ -gon coming from the spin structures.

5 Coamoeba for the mirror of \mathbb{P}^2

The mirror of \mathbb{P}^2 is given by the Laurent polynomial

$$W(x, y) = x + y + \frac{1}{xy}.$$

The critical points of W are given by

$$(x, y) = (1, 1), (\omega, \omega), (\omega^2, \omega^2),$$

where $\omega = \exp(2\pi\sqrt{-1}/3)$ is a primitive cubic root of unity. The corresponding critical values are $3, 3\omega$ and $3\omega^2$. Let $(c_i)_{i=1}^3$ be the distinguished set of vanishing paths obtained as the straight line segments from the origin to the critical values of W as shown in Figure 5.1. The fiber $W^{-1}(0)$ can be realized as a branched double cover of the x -plane by the projection

$$\begin{array}{ccc} \pi : W^{-1}(0) & \rightarrow & \mathbb{C}^{\times} \\ \downarrow \Psi & & \downarrow \Psi \\ (x, y) & \mapsto & x. \end{array}$$

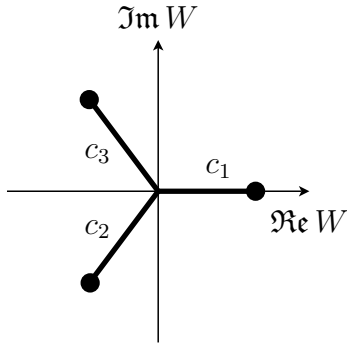


Figure 5.1: A path on the W -plane

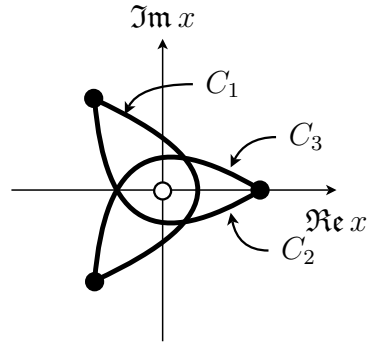


Figure 5.2: The trajectories of the branch points

The branch points of π are given by three dots in Figure 5.2, together with $x = 0$ which does not belong to \mathbb{C}^\times . The fiber $W^{-1}(0)$ can be compactified to an elliptic curve by adding one point over $x = 0$ and two points over $x = \infty$.

Recall that the *coamoeba* of a subvariety of the torus $(\mathbb{C}^\times)^2$ is defined by Passare and Tsikh as its image by the argument map

$$\begin{aligned} \text{Arg} : (\mathbb{C}^\times)^2 &\rightarrow \mathbb{R}^2/\mathbb{Z}^2 \\ \downarrow \quad \downarrow & \\ (x, y) &\mapsto \frac{1}{2\pi}(\arg x, \arg y). \end{aligned}$$

It follows from [28, Theorem 7.1] that the coamoeba of $W^{-1}(0)$ is the union of interiors and vertices of six triangles in Figure 5.3. The inverse image of the set of vertices divide $W^{-1}(0)$ into six triangles as in Figure 5.4. Figures 5.5 and 5.6 show these triangles on two sheets.

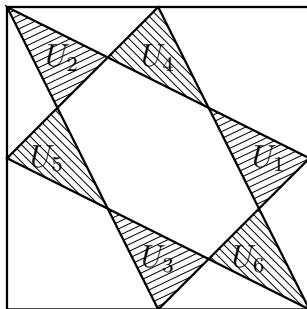


Figure 5.3: The coamoeba of $W^{-1}(0)$

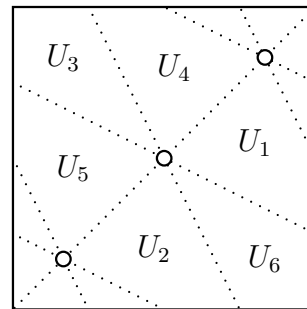


Figure 5.4: The fiber $W^{-1}(0)$

If one deforms $W^{-1}(0)$ to $W^{-1}(c_i(t))$ for $i = 1, 2, 3$ and $t \in [0, 1]$, the branch points move as in Figure 5.2. Here, C_1 , C_2 , and C_3 are trajectories of the branch points along c_1 , c_2 and c_3 respectively. These trajectories are the images of the corresponding vanishing cycles by π up to homotopy. This shows that the vanishing cycles on $W^{-1}(0)$ are as in Figure 5.7. Their images under the argument map are shown in Figure 5.8.

One can see from Figure 5.7 that six triangles in Figure 5.9 are the only polygons on $W^{-1}(0)$ bounded by $\bigcup_i C_i$. By contracting these triangles, one obtains the graph on $W^{-1}(0)$ shown in Figure 5.10. Each of these triangles gives an A_∞ -operation on $\mathfrak{Fut} W$,

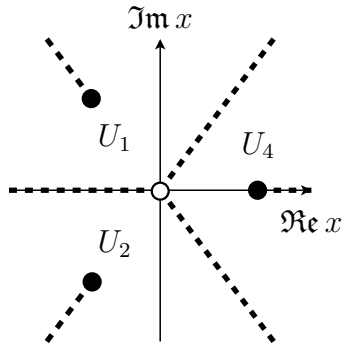


Figure 5.5: The first sheet

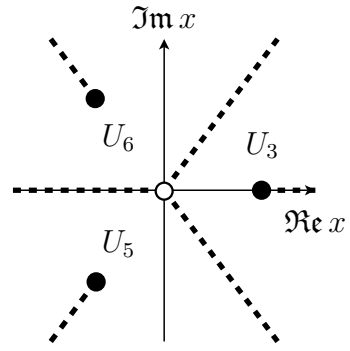


Figure 5.6: The second sheet

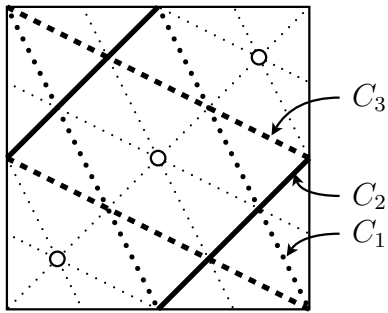


Figure 5.7: Vanishing cycles on $W^{-1}(0)$

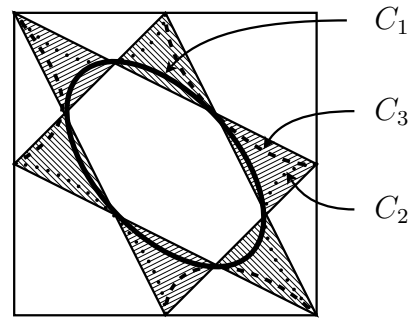


Figure 5.8: Vanishing cycles on the coamoeba

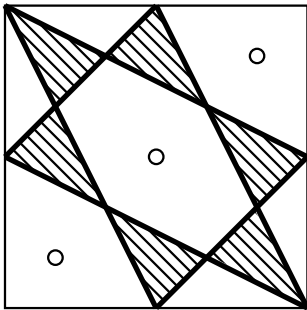


Figure 5.9: Six triangles

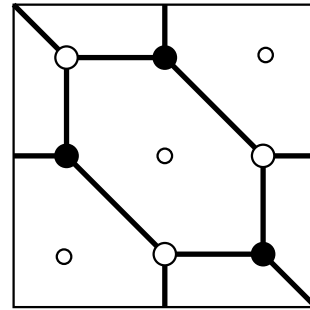


Figure 5.10: A graph on $W^{-1}(0)$

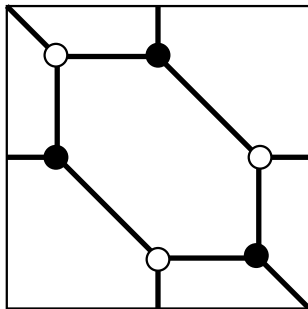


Figure 5.11: A graph on T

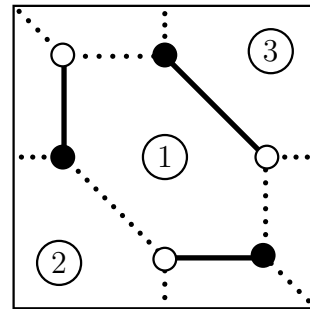


Figure 5.12: The perfect matching

and one can choose the signs so that the contribution of a white node is $+1$, and that of a black node is -1 .

The argument projection G of the graph in Figure 5.10 is shown in Figure 5.11, which is a consistent dimer model. There is a natural bijection between the set of faces of G and the distinguished basis $(C_i)_{i=1}^3$ of vanishing cycles. Moreover, intersections of two vanishing cycles corresponds to common edges of two faces under this bijection.

The order on the distinguished basis of vanishing cycles defines the internal perfect matching in Figure 5.12 by (2.1). In addition, one can choose gradings of C_i so that the Maslov index $\mu(p; C_i, C_j)$ for $p \in C_i \cap C_j$ and $i < j$ is one if the edge corresponding to p is not contained in D , and two otherwise.

This suffices to show the quasi-equivalence

$$\mathcal{A}^\rightarrow \cong \mathfrak{Fuk} W$$

between the directed A_∞ -category associated with the pair (G, D) and the Fukaya category of W . The characteristic polygon of the pair (G, D) coincides with the Newton polygon Δ of W . Since the toric Fano stack X associated with Δ is the projective plane \mathbb{P}^2 , homological mirror symmetry for \mathbb{P}^2 is proved.

6 Dimer models as spines of coamoebas

The discussion in Section 5 motivates the following definition:

Definition 6.1. Let

$$W : \mathbb{T}^\vee \rightarrow \mathbb{C}$$

be a regular map on an algebraic torus $\mathbb{T}^\vee = M \otimes \mathbb{C}^\times = \text{Spec } \mathbb{C}[N]$, G be a consistent dimer model on $T^\vee = M_\mathbb{R}/M$, and D be an internal perfect matching on G . Then the pair (G, D) is said to be *associated with* W if there is a distinguished basis $(C_i)_{i=1}^m$ of vanishing cycles in $W^{-1}(0)$ satisfying the following conditions:

- For any point $p \in W^{-1}(0) \setminus \bigcup_i C_i$, there is at most one polygon bounded by $\bigcup_i C_i$ and passing through p .
- By contracting these polygons, one obtains a bipartite graph Y on $W^{-1}(0)$.
- The restriction of the argument map $\text{Arg} : \mathbb{T}^\vee \rightarrow T^\vee$ to the graph Y is injective.
- The image $\text{Arg}(Y)$ is a consistent dimer model G on T^\vee with respect to a suitable choice of colors on the nodes.
- There is a natural bijection between the set of faces of G and vanishing cycles.
- Intersections of two vanishing cycles corresponds to common edges of two faces under the above bijection.
- The contribution of a polygon in $W^{-1}(0)$ corresponding to a node of G to the A_∞ -operations in $\mathfrak{Fuk} W$ is $+1$ or -1 depending on the color of the node.

- The order on the distinguished basis of vanishing cycles determines an internal perfect matching by (2.1).
- With a suitable choice of gradings on C_i , the Maslov index $\mu(p; C_i, C_j)$ of an intersection $p \in C_i \cap C_j$ for $i < j$ corresponding to an edge e of G is given by

$$\mu(p; C_i, C_j) = \begin{cases} 1 & e \notin D, \\ 2 & e \in D. \end{cases}$$

- The characteristic polygon of the pair (G, D) coincides with the Newton polygon of W .

Now we can state the main conjecture in this paper:

Conjecture 6.2. *Let Δ be a convex lattice polygon in $N_{\mathbb{R}}$ which contains the origin in its interior. Then there exist*

- a Laurent polynomial $W \in \mathbb{C}[N]$ whose Newton polygon coincides with Δ , and
- a pair (G, D) of a consistent dimer model G on T^{\vee} and an internal perfect matching D on G associated with W .

7 Torus-equivariant homological mirror symmetry

In this section, we discuss the relation between dimer models and torus-equivariant homological mirror symmetry for two-dimensional toric Fano stacks. As an example, consider the case when Δ is the convex lattice polygon in Section 5 corresponding to \mathbb{P}^2 and $\phi : N \rightarrow N$ is a linear map represented by the matrix $\begin{pmatrix} 2 & -1 \\ -1 & 2 \end{pmatrix}$. Then $\phi(\Delta)$ is the convex hull of $(2, -1)$, $(-1, 2)$ and $(-1, -1)$ shown in Figure 7.2.

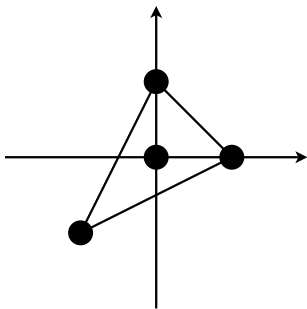


Figure 7.1: The lattice polygon Δ

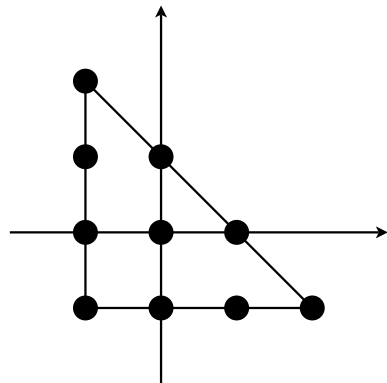


Figure 7.2: The lattice polygon $\phi(\Delta)$

One has

$$K = \text{Ker } \phi \otimes \mathbb{C}^{\times} = \langle (\omega, \omega^2) \rangle \cong \mathbb{Z}/3\mathbb{Z}$$

in this case, where $\omega = \exp(2\pi\sqrt{-1}/3)$ is a primitive cubic root of unity. If we choose

$$W_1(x, y) = x + y + \frac{1}{xy},$$

$$W_2(x, y) = \frac{x^2}{y} + \frac{y^2}{x} + \frac{1}{xy},$$

then the Newton polygons of W_1 and W_2 are given by Δ and $\phi(\Delta)$ respectively, and one has

$$W_2 = W_1 \circ (\psi \otimes \mathbb{C}^\times)$$

where $\psi : M \rightarrow M$ is the transpose of ϕ . Figure 7.3 show the pull-back of the dimer model in Figure 5.11 associated with W_1 by the projection $\pi : M_{\mathbb{R}} \rightarrow T^\vee$, and the dimer model associated with W_2 is obtained as its quotient by the lattice $\psi(M)$ generated by $(2, -1)$ and $(-1, 2)$. The resulting dimer model is shown in Figure 7.4, which is a covering of the former with the group of characters of K as the group of deck transformations.

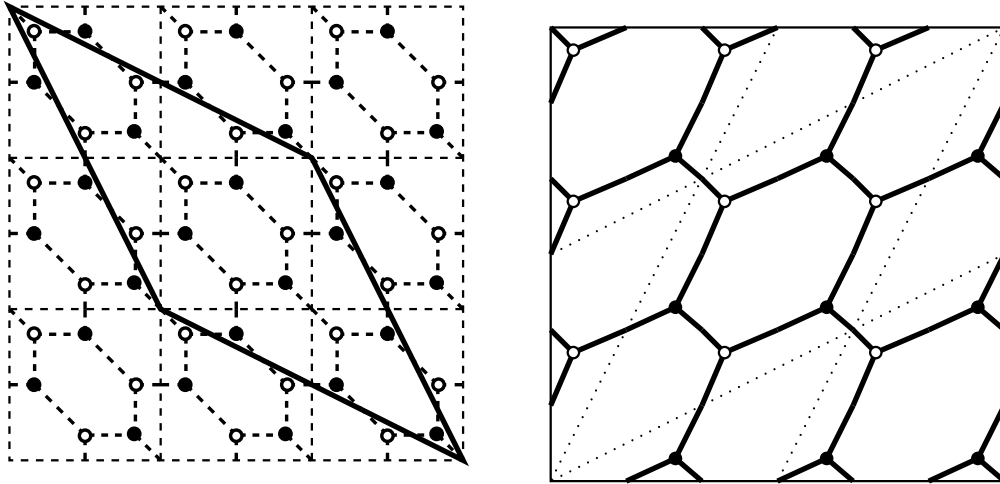


Figure 7.3: The pull-back by π of the dimer model associated with W_1 and a fundamental region of the action by the lattice $\psi(M)$

Figure 7.4: A dimer model associated with W_2

Figure 7.5 shows the correspondence between fundamental regions of the M -action and characters of the torus \mathbb{T} . The operation of taking the quotient with respect to the action of $\psi(M)$ corresponds to the restriction of characters to $K \subset \mathbb{T}$, and the resulting characters of K are shown in Figure 7.6.

By comparing Figures 5.12, 7.3 and 7.6, one can label faces of the dimer model in Figure 7.4 as in Figure 7.7; the face labeled as $\binom{i}{j}$ corresponds to the j -th lift to $W_2^{-1}(0)$ of the vanishing cycle C_i of W_1 .

The fiber $W_2^{-1}(0)$ of W_2 can be obtained by assigning a triangle to each node in Figure 7.8 and gluing them together as in Figure 7.9. Vanishing cycles on the resulting elliptic curve minus nine points are shown in Figure 7.10.

As the distinguished basis (C_1, C_2, C_3) of vanishing cycles of W_1 corresponds to the full exceptional collection

$$(E_1, E_2, E_3) = (\Omega_{\mathbb{P}^2}^2(2)[2], \Omega_{\mathbb{P}^2}^1(1)[1], \mathcal{O}_{\mathbb{P}^2})$$

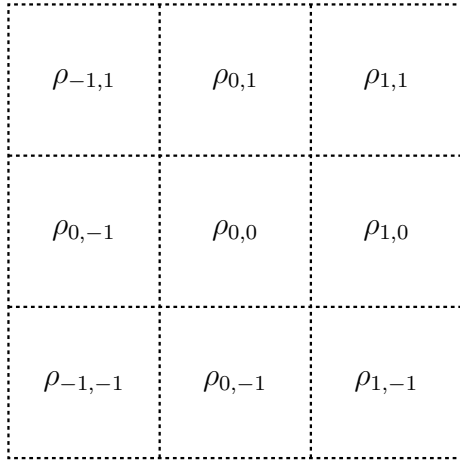


Figure 7.5: Characters of \mathbb{T}

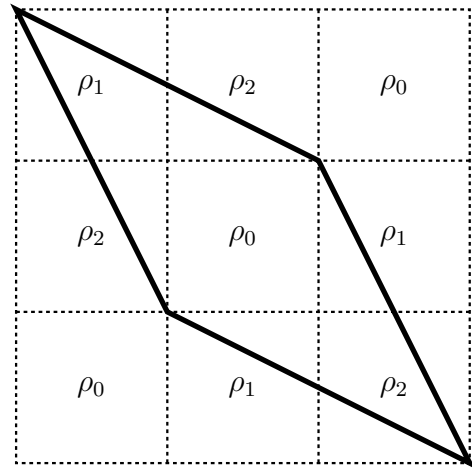


Figure 7.6: Characters of K

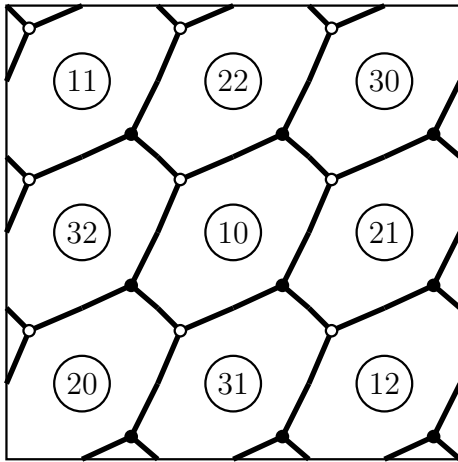


Figure 7.7: Labels on the faces

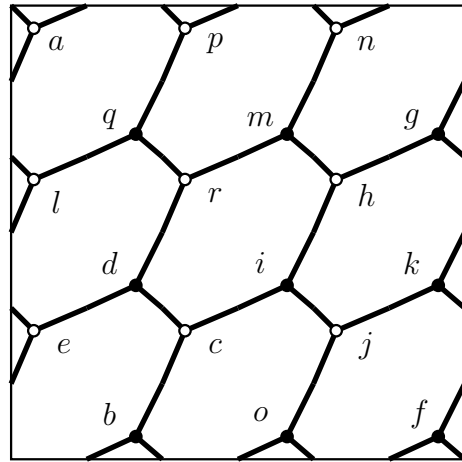


Figure 7.8: Labels on the nodes

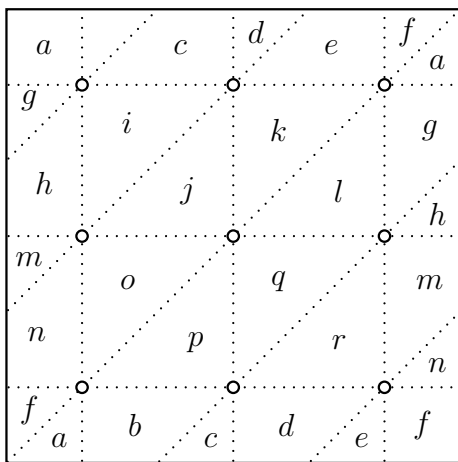


Figure 7.9: The fiber $W_2^{-1}(0)$

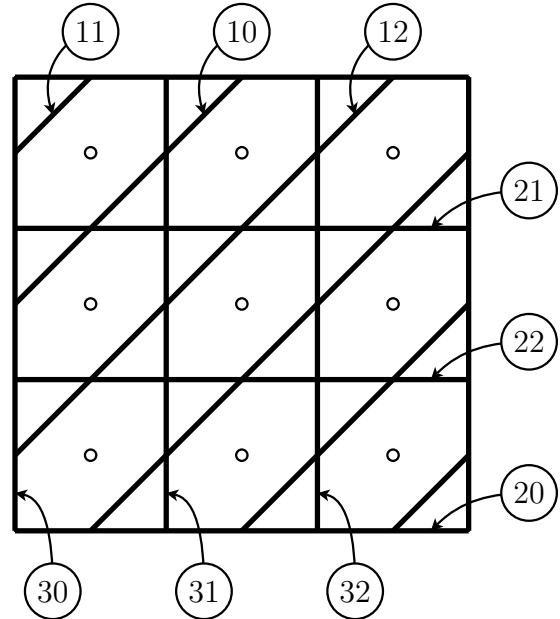


Figure 7.10: Vanishing cycles on $W_2^{-1}(0)$

by homological mirror symmetry, the vanishing cycle \textcircled{ij} of W_2 corresponds to the object $E_i \otimes \rho_j$ in $D^b \text{coh}[\mathbb{P}^2/K] \cong D^b \text{coh}^K \mathbb{P}^2$. In this way, the pair (G, D) associated with W_1 encodes homological mirror symmetry for any subgroup of the torus \mathbb{T} acting on \mathbb{P}^2 .

In general, if a pair (G, D) is associated with W , then the pair $((\psi \otimes (\mathbb{R}/\mathbb{Z}))^{-1}(G), ((\psi \otimes (\mathbb{R}/\mathbb{Z}))^{-1}(D))$ obtained as the pull-back by the map

$$\psi \otimes (\mathbb{R}/\mathbb{Z}) : T^\vee \rightarrow T^\vee$$

is associated with the pull-back $W \circ (\psi \otimes \mathbb{C}^\times)$ of W by the map

$$\psi \otimes \mathbb{C}^\times : \mathbb{T}^\vee \rightarrow \mathbb{T}^\vee.$$

This immediately implies Theorem 1.2 and Theorem 1.3.

8 Toric del Pezzo surfaces

We prove Theorem 1.4 in this section. We first discuss the case when X is \mathbb{P}^2 blown-up at one point. The corresponding lattice polygon Δ is the convex hull of

$$v_1 = (1, 0), v_2 = (0, 1), v_3 = (-1, 0), \text{ and } v_4 = (-1, -1).$$

A Laurent polynomial

$$W(x, y) = x + y - \frac{1}{x} + \frac{1}{xy},$$

whose Newton polygon coincides with Δ , has four critical points. Take the origin as the base point and let $(c_i)_{i=1}^4$ be the distinguished set of vanishing paths, defined as the straight line segments from the origin to the critical values as in Figure 8.1. Consider the second projection

$$\begin{array}{ccc} \pi : W^{-1}(0) & \rightarrow & \mathbb{C}^\times \\ \cup & & \cup \\ (x, y) & \mapsto & y. \end{array}$$

The fiber $\pi^{-1}(y)$ consists of two points for $y \in \mathbb{C}^\times \setminus \{1\}$, whereas $\pi^{-1}(1)$ consists of only one point (the other point goes to $x = 0$). Figure 8.2 shows the image by π of the distinguished basis $(C_i)_{i=1}^4$ of vanishing cycles along the paths $(c_i)_{i=1}^4$. The black dots are the branch points, the white dots are $y = 0$ and $y = 1$, the solid lines are the images of the vanishing cycles and the dotted lines are cuts introduced artificially to divide $W^{-1}(0)$ into two sheets as shown in Figure 8.5 and Figure 8.6.

Unlike the case of \mathbb{P}^2 discussed in Section 5, the actual boundary of the coamoeba does not coincide with the asymptotic boundary. Figure 8.3 shows a schematic picture of the coamoeba. To study the image of the vanishing cycles by the argument map, we cut the coamoeba into pieces along the bold lines in Figure 8.4. These lines look as in Figure 8.5 and Figure 8.6 on the two sheets. They cut $W^{-1}(0)$ into the union of two quadrilaterals and four triangles, glued along ten edges. By gluing these pieces, one obtains an elliptic curve minus four points in Figure 8.7. One can see that the vanishing cycles on $W^{-1}(0)$ looks as in Figure 8.8 using Figures 8.2, 8.5, 8.6, and 8.7.

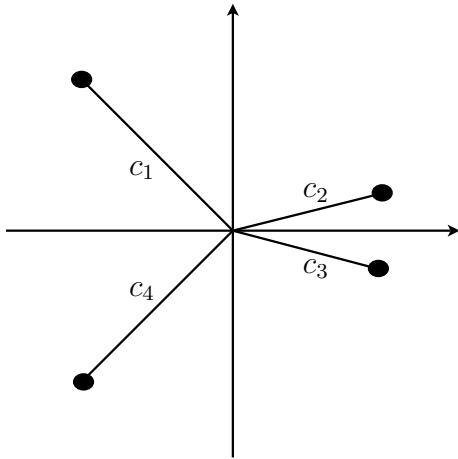


Figure 8.1: A distinguished basis of vanishing paths

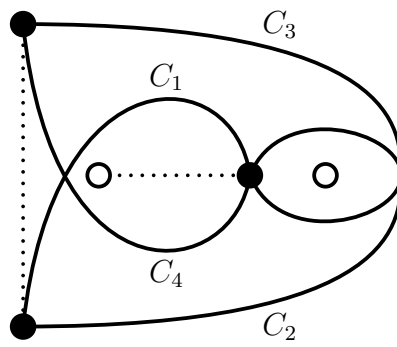


Figure 8.2: The images by π of the vanishing cycles

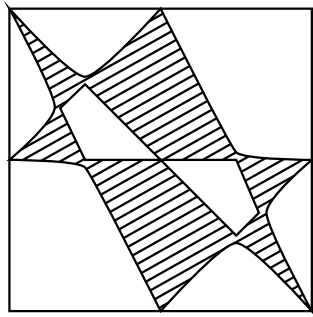


Figure 8.3: The coamoeba of $W^{-1}(0)$

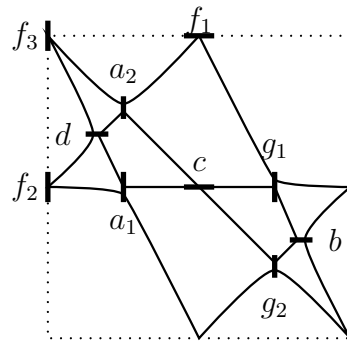


Figure 8.4: Cutting the coamoeba into pieces

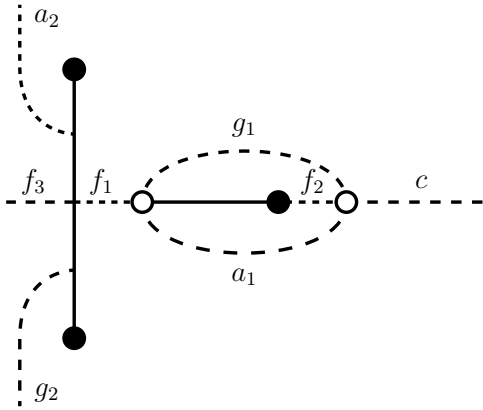


Figure 8.5: The first sheet of $W^{-1}(0)$

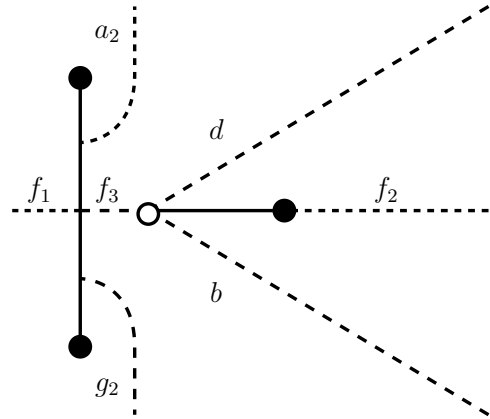


Figure 8.6: The second sheet of $W^{-1}(0)$

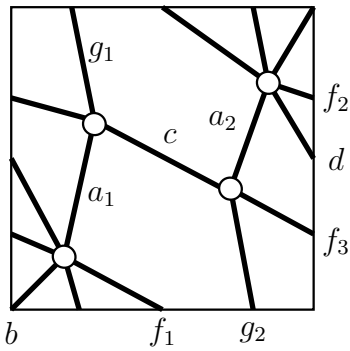


Figure 8.7: The glued surface

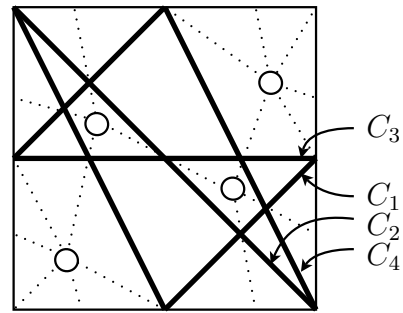


Figure 8.8: The vanishing cycles

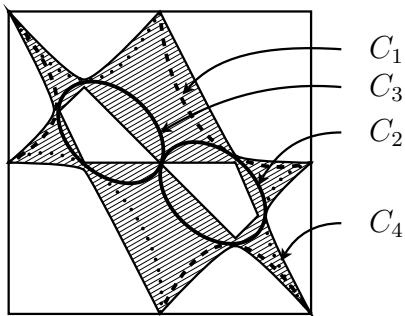


Figure 8.9: Vanishing cycles on the coamoeba

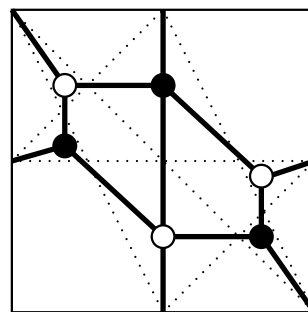


Figure 8.10: The dimer model

One can also see that the images of the vanishing cycles by the argument map encircle the holes in the coamoeba as shown in Figure 8.9. Now it is easy to see that Conjecture 6.2 holds in this case.

The case of $\mathbb{P}^1 \times \mathbb{P}^1$ is proved in [27]. The case of \mathbb{P}^2 blown-up at two or three points are completely parallel to the case of \mathbb{P}^2 blown-up at one point discussed above, and we omit the detail here.

References

- [1] Mohammed Abouzaid. Homogeneous coordinate rings and mirror symmetry for toric varieties. *Geom. Topol.*, 10:1097–1157 (electronic), 2006.
- [2] Mohammed Abouzaid. Morse homology, tropical geometry, and homological mirror symmetry for toric varieties. *Selecta Math. (N.S.)*, 15(2):189–270, 2009.
- [3] Denis Auroux, Ludmil Katzarkov, and Dmitri Orlov. Mirror symmetry for del Pezzo surfaces: vanishing cycles and coherent sheaves. *Invent. Math.*, 166(3):537–582, 2006.
- [4] Denis Auroux, Ludmil Katzarkov, and Dmitri Orlov. Mirror symmetry for weighted projective planes and their noncommutative deformations. *Ann. of Math. (2)*, 167(3):867–943, 2008.
- [5] Bohan Fang. Homological mirror symmetry is T -duality for \mathbb{P}^n . *Commun. Number Theory Phys.*, 2(4):719–742, 2008.
- [6] Bohan Fang, Chiu-Chu Melissa Liu, David Treumann, and Eric Zaslow. The coherent-constructible correspondence and homological mirror symmetry for toric varieties. arXiv:0901.4276.
- [7] Bohan Fang, Chiu-Chu Melissa Liu, David Treumann, and Eric Zaslow. The coherent-constructible correspondence for toric orbifolds. arXiv:0911.4711.
- [8] Bo Feng, Yang-Hui He, Kristian D. Kennaway, and Cumrun Vafa. Dimer models from mirror symmetry and quivering amoebae. *Adv. Theor. Math. Phys.*, 12(3):489–545, 2008.
- [9] Sebastián Franco, Amihay Hanany, Dario Martelli, James Sparks, David Vegh, and Brian Wecht. Gauge theories from toric geometry and brane tilings. *J. High Energy Phys.*, (1):128, 40 pp. (electronic), 2006.
- [10] Sebastián Franco, Amihay Hanany, David Vegh, Brian Wecht, and Kristian D. Kennaway. Brane dimers and quiver gauge theories. *J. High Energy Phys.*, (1):096, 48 pp. (electronic), 2006.
- [11] Sebastián Franco and David Vegh. Moduli spaces of gauge theories from dimer models: proof of the correspondence. *J. High Energy Phys.*, (11):054, 26 pp. (electronic), 2006.

- [12] Masahiro Futaki and Kazushi Ueda. Exact Lefschetz fibrations associated with dimer models. arXiv:0912.1656.
- [13] Amihay Hanany, Christopher P. Herzog, and David Vegh. Brane tilings and exceptional collections. *J. High Energy Phys.*, (7):001, 44 pp. (electronic), 2006.
- [14] Amihay Hanany and Kristian D. Kennaway. Dimer models and toric diagrams. hep-th/0503149, 2005.
- [15] Amihay Hanany and David Vegh. Quivers, tilings, branes and rhombi. *J. High Energy Phys.*, (10):029, 35, 2007.
- [16] Akira Ishii and Kazushi Ueda. Dimer models and exceptional collections. arXiv:0911.4529.
- [17] Gabriel Kerr. Weighted blowups and mirror symmetry for toric surfaces. *Adv. Math.*, 219(1):199–250, 2008.
- [18] Maxim Kontsevich. Homological algebra of mirror symmetry. In *Proceedings of the International Congress of Mathematicians, Vol. 1, 2 (Zürich, 1994)*, pages 120–139, Basel, 1995. Birkhäuser.
- [19] Maxim Kontsevich. Lectures at ENS Paris, spring 1998. set of notes taken by J. Bellaïche, J.-F. Dat, I. Martin, G. Rachinet and H. Randriambololona, 1998.
- [20] Sergey Mozgovoy and Markus Reineke. On the noncommutative Donaldson-Thomas invariants arising from brane tilings. arXiv:0809.0117.
- [21] Kyoji Saito. Around the theory of the generalized weight system: relations with singularity theory, the generalized Weyl group and its invariant theory, etc. [MR0855023 (88c:32015a); MR0876442 (88c:32015b)]. In *Selected papers on harmonic analysis, groups, and invariants*, volume 183 of *Amer. Math. Soc. Transl. Ser. 2*, pages 101–143. Amer. Math. Soc., Providence, RI, 1998.
- [22] Paul Seidel. More about vanishing cycles and mutation. In *Symplectic geometry and mirror symmetry (Seoul, 2000)*, pages 429–465. World Sci. Publishing, River Edge, NJ, 2001.
- [23] Paul Seidel. Vanishing cycles and mutation. In *European Congress of Mathematics, Vol. II (Barcelona, 2000)*, volume 202 of *Progr. Math.*, pages 65–85. Birkhäuser, Basel, 2001.
- [24] Paul Seidel. Homological mirror symmetry for the quartic surface. math.AG/0310414, 2003.
- [25] Paul Seidel. *Fukaya categories and Picard-Lefschetz theory*. Zurich Lectures in Advanced Mathematics. European Mathematical Society (EMS), Zürich, 2008.
- [26] Kazushi Ueda. Homological mirror symmetry for toric del Pezzo surfaces. *Comm. Math. Phys.*, 264(1):71–85, 2006.

- [27] Kazushi Ueda and Masahito Yamazaki. Dimer models for parallelograms. math.AG/0606548.
- [28] Kazushi Ueda and Masahito Yamazaki. A note on dimer models and McKay quivers. math.AG/0605780.

Kazushi Ueda

Department of Mathematics, Graduate School of Science, Osaka University, Machikaneyama 1-1, Toyonaka, Osaka, 560-0043, Japan.

e-mail address : kazushi@math.sci.osaka-u.ac.jp

Masahito Yamazaki

Department of Physics, Graduate School of Science, University of Tokyo, Hongo 7-3-1, Bunkyo-ku, Tokyo, 113-0033, Japan

e-mail address : yamazaki@hep-th.phys.s.u-tokyo.ac.jp